PROCEEDINGS OF SCIENCE

Gluon propagators near the phase transition in $SU(2)$ gluodynamics

V.G. Bornyakov[*†]
School of Biomedicine, Far Eastern Federal University, 690950 Vladivostok, Russia,
Institute for High Energy Physics, NRC "Kurchatov Institutei", 142281 Protvino, Russia,
Institute of Theoretical and Experimental Physics, 117259 Moscow, Russia
E-mail: vitaly.bornyakov@ihep.ru

V.K. Mitrjushkin
Joint Institute for Nuclear Research, 141980 Dubna, Russia
and Institute of Theoretical and Experimental Physics, 117259 Moscow, Russia
E-mail: vmitr@theor.jinr.ru

R.N. Rogalyov
Institute for High Energy Physics, NRC "Kurchatov Institutei", 142281 Protvino, Russia,
School of Biomedicine, Far Eastern Federal University, 690950 Vladivostok, Russia
E-mail: Roman.Rogalyov@ihep.ru

We study numerically the $SU(2)$ Landau gauge transverse and longitudinal gluon propagators at non-zero temperatures T of the phase transition. Our goal is to provide high precision estimates of these propagators free of finite volume and Gribov copy systematic effects and with small scaling violations. We compute the electric screening mass and the asymmetry of the dimension two condensate and study their behavior near criticality.

The 33rd International Symposium on Lattice Field Theory
14 -18 July 2015
*Kobe International Conference Center, Kobe, Japan**

*Speaker.

†This work was supported by the grants RFBR 13-02-01387a and 14-02-01185a.

PoS(LATTICE 2015)321

1. Introduction

The gluon propagator being gauge dependent quantity is still of fundamental importance. The nonperturbative computation of this quantity is needed to guide the Dyson–Schwinger equation (DSE) practitioners with the correct choice of truncation of this infinite set of equations. It is also believed that the gluon propagator determines the mass scale which is often called effective gluon mass and which is gauge invariant. Such mass is especially important at finite temperature when it plays the role of the screening mass. Lattice computations of the gluon propagator provide a possibility to compute this quantity from the first principles keeping systematic errors under control. For this reason, lattice results are often used as an input for DSE studies, especially at small momenta where modern methods to solve DSE do not provide reliable results.

In this paper we compute the gluon propagators in the Landau gauge in $SU(2)$ lattice gluodynamics close to the phase transition from the confinement to the deconfinement phase.

We obtain results free of Gribov copy effects and make an extrapolation to the infinite volume limit. Our results are obtained at small lattice spacing $a \approx 0.1$fm so we can consider finite lattice spacing effects to be small.

There are two opposite opinions about behavior of the electric gluon propagator $D_L(p)$ at the phase transition of $SU(2)$ gluodynamics. In [3, 4] where lattices with $N_t = 4$ and 6 were used, it was shown that the screening mass extracted from the propagator $D_L(p)$ showed specific critical behavior in the vicinity of the transition temperature. In [5] where lattices with large N_t up to $N_t = 16$ were studied conclusion was made that there is no specific signature of deconfinement associated with $D_L(p)$, i.e., the effects observed in [3, 4] are just lattice artifacts.

2. Gauge fixing and extrapolation to the infinite volume limit

We employ the gauge fixing procedure used earlier in our study of the gluon propagator at finite temperature [1]. In the gauge fixing procedure we employ the $Z(2)$ flip operation proposed in [7]. $Z(2)$ flip in direction μ consists in flipping all link variables $U_{x\mu}$ attached and orthogonal to a 3d plane by multiplying them with -1. Such global flips are equivalent to non-periodic gauge transformations and represent an exact symmetry of the pure gauge action. The Polyakov loops in the direction of the chosen links and averaged over the 3d plane obviously change their sign. At finite temperatures we apply flips only to directions $\mu = 1,2,3$. In the deconfinement phase, where the $Z(2)$ symmetry is broken, the $Z(2)$ sector of the Polyakov loop in the $\mu = 4$ direction has to be chosen since on large enough volumes all lattice configurations belong to the same sector, i.e. there are no flips between sectors in the Markov chain of configurations. We choose the sector with positive Polyakov loop. In the confinement phase one may use a flip in the $\mu = 4$ direction. However, in [1] it was found that the maximal gauge fixing functional was obtained in the positive Polyakov loop sector in more than 90 % cases. To save computer time we stick to this sector for all configurations in the confinement phase. Therefore, in our study the flip operations combine for each lattice field configuration the 2^3 distinct gauge orbits (or Polyakov loop sectors) of strictly periodic gauge transformations into one larger gauge orbit.

We find rather strong finite-volume effects for the propagators over the subcritical domain. They are substantial throughout the whole infrared domain ($p < 1$ GeV), as is seen in Fig. 1.

Therefore, we needed to make extrapolation to the infinite volume. As for the transverse propagator, it is plagued by Gribov-copy effects and shows only a weak temperature dependence near T_c. Here we focus our attention on the longitudinal propagator.

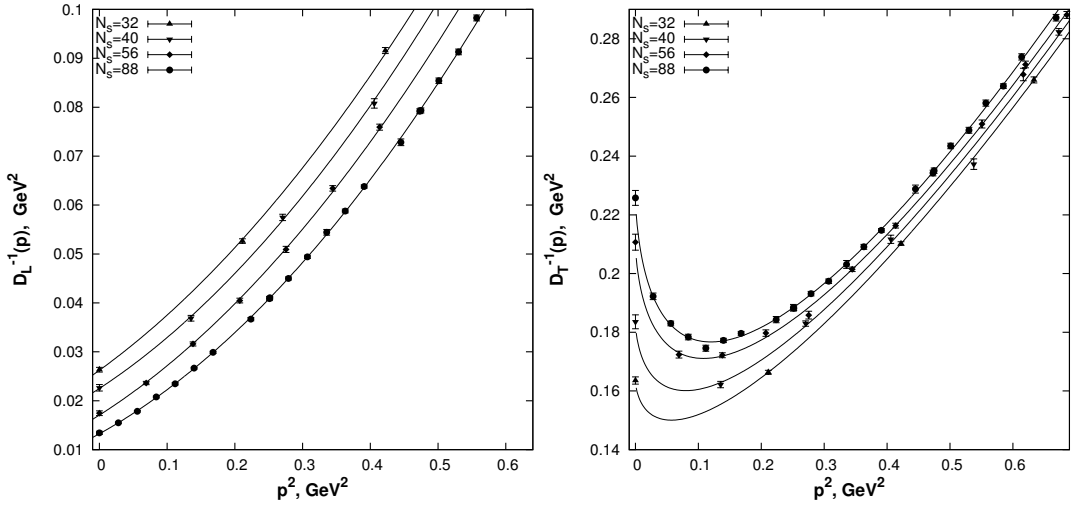

Figure 1: Inverse longitudinal (left panel) and transverse (right panel) propagators as functions of the momentum at various lattice sizes, $T/T_c = 0.98602$; only the case of zero Matsubara frequency $p_4 = 0$ is considered. At $\vec{p} \neq 0$, the quantinites D_L and D_T are defined by the formulas $D_L(\vec{p},0) = \dfrac{a^4}{3}\sum_{x,b} e^{i\vec{p}\vec{x}}\langle A_4^b(x)A_4^b(0)\rangle$, $D_T(\vec{p},0) = \dfrac{a^4}{6}\sum_{i=1}^{3}\sum_{x,b} e^{i\vec{p}\vec{x}}\langle A_i^b(x)A_i^b(0)\rangle$, where $A_\mu^b(x) = Tr\left[(U_{x,\mu} - U_{x,\mu}^\dagger)\sigma^b\right]/2iag$.

In principle, we can approach the infinite-volume limit in two steps. First, we fix N_s and determine $D_L(p;N_s)$ using only the data at a given value of N_s. Then we find $D_L(p;N_s=\infty)$ using a fit function of the type

$$D_L^{-1}(p;N_s) \simeq a_0 + \frac{a_1}{N_s} + \frac{a_2}{N_s^2} + ... \tag{2.1}$$

In this case, the quantities $D_L(p;N_s)$ at a given value of p and different values of N_s are thought of as independent and correaltions between them are ignored. Therefore, some information is lost and the errors in $D_L(p;N_s=\infty)$ are overestimated.

For this reason, we use a combined fit over $1/N_s$ and p for a restricted range of p. We fit the inverse longitudinal propagator $D_L^{-1}(p;N_s)$ by a function of the form

$$\begin{aligned} f_A(p;N_s) \;=\; & c_{00} + c_{10}p_\sigma^2 + c_{20}(p_\sigma^2)^2 + ... \\ & + c_{01}\frac{1}{\lambda} + c_{11}\frac{p_\sigma^2}{\lambda} + c_{21}\frac{p_\sigma^4}{\lambda} + ... \\ & + c_{02}\frac{1}{\lambda^2} + c_{12}\frac{p_\sigma^2}{\lambda^2} + c_{22}\frac{p_\sigma^4}{\lambda^2} + ... \end{aligned} \tag{2.2}$$

where we introduced dimensionless variables $p_\sigma = \dfrac{p}{\sqrt{\sigma}}$ and $\lambda = N_s a \cdot T_c = \dfrac{N_s}{N_t \xi}$, $\xi = \dfrac{T}{T_c}$ and subscript A labels the fit name. A combined fit involves a greater number of data points, thus

statistical criteria work better. The use of the polynomial dependence on p^2 in (2.2) is motivated by results of Refs. [1] and [2].

We considered fit functions (2.2) with the number of parameters varying from 6 to 11. and employ the regression analysis to choose the optimal fit. To illustrate this procedure, we compare fits with 9 ($A=Q$) and 7 ($A=J$) parameters for $40 \le N_s \le 88$ and $0 < p < 1$ GeV.

First we compute $\chi^2(A) = \sum_{p_\sigma,\lambda} \frac{\left(D_L^{-1}(p_\sigma,\lambda) - f_A(p_\sigma,\lambda;\vec{\theta})\right)^2}{\delta(p_\sigma,\lambda)^2}$ for each fit $A = Q, J$;

here $\vec{\theta}$ is the vector of the parameters; $\vec{\theta} = (c_{00}, c_{10}, c_{20}, c_{30}, c_{01}, c_{11}, c_{21})$ for the fit J and $\vec{\theta} = (c_{00}, c_{10}, c_{20}, c_{30}, c_{01}, c_{11}, c_{21}, c_{12}, c_{22})$ for the fit Q (see formula (2.2)).

Now we compare fit functions f_Q and f_J depending on n_Q and n_J parameters, respectively ($n_Q > n_J$). If the data sample has N points ($N = \sum_{p_\sigma,\lambda} 1$) then the distribution of the quantity (referred to as the Fisher variable)

$$f = \frac{\left[(\chi^2(J) - \chi^2(Q))/(n_Q - n_J)\right]}{\left[\chi^2(Q)/(N - n_Q)\right]} \tag{2.3}$$

should be compared with the Fisher distribution, whose probability density function $\mathscr{P}_{n_Q - n_J, N - n_Q}(z)$ is defined by the formula

$$\mathscr{P}_{2p,2q}(z) = \frac{\Gamma(p+q)}{\Gamma(p)\Gamma(q)} \frac{p^p q^q z^{p-1}}{(q+pz)^{p+q}}, \qquad z \ge 0. \tag{2.4}$$

In the case $p = 1, q \gg 1, q \gg f$ the respective cumulative distribution function (CDF) $F_{th}(z) = \int_0^z \mathscr{P}(x)dx$ can be approximated by $\tilde{F}_{th}(z) = 1 - \exp(-z)$, which is independent of q. In the case under consideration, $n_J = 7$, $n_Q = 9$, $N \simeq 100$ and all requared conditions are fulfiled.

If the variable f is Fisher distributed then both fit functions work well and the J fit should be chosen because it involves less number of the parameters. Otherwise (if f lies far on a tail of the Fisher distribution) the quality of the Q fit is better than that of the J fit.

We compare theoretical and empirical CDF and employ the Kolmogorov-Smirnov test based on the theorem that, as $N \to \infty$, the random variable $x = \sqrt{N} \sup_f |F_N(f) - F_{theor}(f)|$ is Kolmogorov distributed with the CDF $K(x) = \sum_{j=-\infty}^{\infty} (-1)^j e^{-2j^2x^2}$.

In the case under consideration, $|F_N(f) - F_{theor}(f)|$ approaches its peak (0.531) at $f = 1.996$, $N = 12$, therefore, $x = 1.839$ and $K(x) = 0.997$; thus we arrive at the conclusion that the Q fit is better than the J fit with the p-value≈ 0.003.

3. Screening masses

The first computation of the electric screening mass m_E from the longitudinal gluon propagator in momentum space $D_L(p)$ was presented in Ref. [1] for $SU(2)$ theory. The electric screening mass is conventionally defined in terms of the longitudinal propagator, $M = 1/\sqrt{D_L(0)}$. Thus it depends on the normalization condition. The authors of [3, 4, 2] used the normalization condition

$$D_L^{MOM}(p^2 = \mu^2) = \frac{1}{\mu^2}, \tag{3.1}$$

referred to as the MOM normalization; the authors of [1, 6, 2] used the so called on-mass-shell (OMS) normalization defined by the formula

$$\frac{1}{D_L^{OMS}(p)} = M_{OMS}^2 + p^2 + \underline{O}(p^4). \tag{3.2}$$

The respective renormalization factors are defined by

$$D_L^{MOM}(p) = Z_{MOM} D_L^{bare}(p); \quad D_L^{OMS}(p) = Z_{OMS} D_L^{bare}(p) \tag{3.3}$$

where $D_L^{bare}(p) = D_L(p)$ is the unrenormalized propagator obtained from simulations (see the caption to Fig.1).

In the infinite-volume limit, $D_L^{OMS}(0) = c_{10}/c_{00}$ has unappropriately large errors of extrapolation due to uncertainty in c_{10} and we don't consider it here. $D_L^{MOM}(p)$ behaves similar to $D_L^{bare}(p)$ because Z_{MOM} has only a weak dependence on the temperature. Thus we focus our attention on $D_L^{MOM}(p)$.

Since M_{MOM} has a minimum close to T_c but definitely below it, $D_L(0)$ takes its maximum below T_c.

To clarify the question of critical behavior, we consider $M_{MOM}(\xi)$ over the range[1] $0.99 < \xi < 1.06$ and fit it to the following function:

$$\xi < d: \quad M_{MOM} \simeq a - q(d-\xi)^b; \tag{3.4}$$

$$\xi > d: \quad M_{MOM} \simeq a + c(\xi - d)^b. \tag{3.5}$$

The results of this 5-parameter fit with 5 degrees of freedom are presented in Fig. 2. Therewith, we can assume a polynomial dependence of M_{MOM} on the temperature, see Fig. 2.

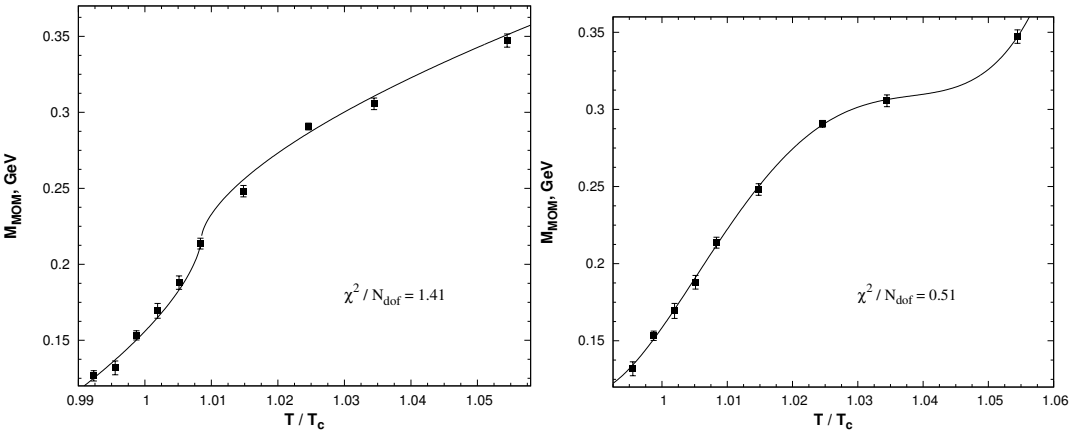

Figure 2: Parameters obtained in the fit: $a = 0.217(3)$ **GeV;** $d = 1.0085(3)$**;** $b = 0.63(3)$**;** $c = 0.93(11)$ **GeV;** $q = 1.23(19)$ **GeV.** The fit describing critical behavior shown in the left panel is compared to the polynomial fit describing smooth behavior in the right panel.

However, a more detailed analysis may be required. The results of the extrapolation to the infinite-volume limit can depend on the domain in the $p_\sigma - \lambda$ plane over which our fit is performed.

[1] We use the notation $\xi = T/T_c$.

The error associated with the choice of this domain was taken into account only partially: we varied the upper cutoff momentum over the range 0.9 GeV $< p_{cut} <$ 1.1 GeV and found that the dependence on such variations can be neglected. For a more thorough extrapolation larger statistics is needed.

4. $\langle A^2 \rangle$ asymmetry

Studies of the dimension two condensate $\langle A^2 \rangle$ in gauge theories were started in Ref. [8], where it was shown that it measures topological structures responsible for the confinement-deconfinement transition in the compact electrodynamics. In the last years this condensate has received considerable attention (see e.g. [9], and references therein). It plays an important role in the studies of the infrared properties of the Yang–Mills theories.

The $\langle A^2 \rangle$ condensate is defined as

$$\langle A^2 \rangle = g^2 \langle A^a_\mu(x) A^a_\mu(x) \rangle. \tag{4.1}$$

At nonzero temperature one can consider two condensates

$$\langle A^2_E \rangle = g^2 \langle A^a_4(x) A^a_4(x) \rangle, \qquad \langle A^2_M \rangle = g^2 \langle A^a_i(x) A^a_i(x) \rangle.$$

The $\langle A^2 \rangle$ asymmetry introduced in Ref. [10] is defined as

$$\Delta_{A^2} \equiv < A^2_E > - \frac{1}{3} < A^2_M > . \tag{4.2}$$

The asymmetry is ultraviolate finite [10],[11].

The quantity Δ_{A^2} was studied numerically in Ref. [10] at low and high temperature as well as near the phase transition. Here we only consider vicinity of the phase transition. For this range of temperature it was found in [10] that has a sharp maximum at the temperature $T \approx T_c$. The location of the maximum T_{max} was determined as $T_{max} = 1.00(3) T_c$.

We compute Δ_{A^2} on the same set of lattices as was used above for propagators $D_{L,T}(p)$ computations. We find $T_{max}/T_c = 0.979(5)$, i.e. the maximum of Δ_{A^2} is below T_c.

We find that, in the region around T_c, Δ_{A^2} shows behavior analogous to that of M_{MOM}. To describe this behavior we employ the fit function:

$$\xi < d: \quad \Delta_{A^2} = a + q(d - \xi)^b; \tag{4.3}$$

$$\xi > d: \quad \Delta_{A^2} = a - c(\xi - d)^b. \tag{4.4}$$

This 5-parameter fit performed over the range $0.99 < \xi < 1.06$ (10 data points) gives $\chi^2/N_{d.o.f.} = 1.00$ and parameters

$$d = 1.0085 \pm 0.0007, \qquad a = 2.59 \pm 0.09, \tag{4.5}$$

$$c = 6.59 \pm 0.58, \qquad q = 25.14 \pm 6.04, \tag{4.6}$$

$$b = 0.62 \pm 0.05. \tag{4.7}$$

We compare the fit function (4.3, 4.4) with the 5-parameter polynomial fit function

$$P(\xi) = r_0 + r_1 \xi + r_2 \xi^2 + r_3 \xi^3 + r_4 \xi^4, \tag{4.8}$$

see Fig.3, right panel. Here we obtain $\frac{\chi^2}{N_{d.o.f.}} = 2.72$, the corresponding p-value $= 1.9\%$ as contrasted to the p-value $= 42\%$ in the case of fit function (4.3, 4.4). This comparison gives support to the critical behavior of Δ_{A^2}.

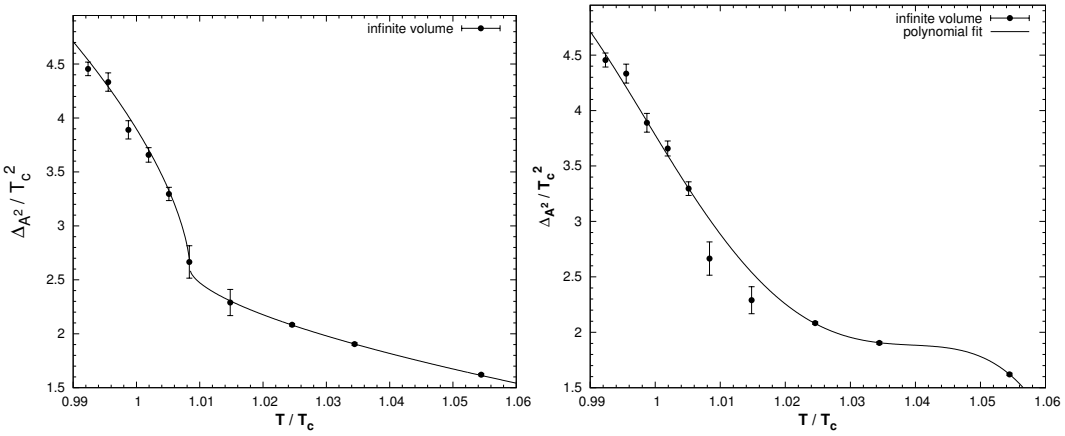

Figure 3: Comparison of two fits: (4.3, 4.4) versus (4.8)

References

[1] V. G. Bornyakov and V. K. Mitrjushkin, Phys. Rev. D **84** (2011) 094503 [arXiv:1011.4790 [hep-lat]].

[2] P. J. Silva, O. Oliveira, P. Bicudo and N. Cardoso, Phys. Rev. D **89**, no. 7, 074503 (2014) [arXiv:1310.5629 [hep-lat]].

[3] C. S. Fischer, A. Maas and J. A. Muller, Eur. Phys. J. C **68**, 165 (2010) [arXiv:1003.1960 [hep-ph]].

[4] A. Maas, J. M. Pawlowski, L. von Smekal and D. Spielmann, Phys. Rev. D **85**, 034037 (2012) [arXiv:1110.6340 [hep-lat]].

[5] A. Cucchieri and T. Mendes, Acta Phys. Polon. Supp. **7**, no. 3, 559 (2014). doi:10.5506/APhysPolBSupp.7.559

[6] V. G. Bornyakov and V. K. Mitrjushkin, Int. J. Mod. Phys. A **27** (2012) 1250050 [arXiv:1103.0442 [hep-lat]].

[7] I. L. Bogolubsky, V. G. Bornyakov, G. Burgio, E. M. Ilgenfritz, M. Muller-Preussker and V. K. Mitrjushkin, Phys. Rev. D **77**, 014504 (2008) [Phys. Rev. D **77**, 039902 (2008)] doi:10.1103/PhysRevD.77.014504, 10.1103/PhysRevD.77.039902 [arXiv:0707.3611 [hep-lat]].

[8] F. V. Gubarev, L. Stodolsky and V. I. Zakharov, Phys. Rev. Lett. **86**, 2220 (2001) doi:10.1103/PhysRevLett.86.2220 [hep-ph/0010057].

[9] M. A. L. Capri, D. Dudal, J. A. Gracey, V. E. R. Lemes, R. F. Sobreiro, S. P. Sorella and H. Verschelde, Phys. Rev. D **72**, 105016 (2005) doi:10.1103/PhysRevD.72.105016 [hep-th/0510240].

[10] M. N. Chernodub and E.-M. Ilgenfritz, Phys. Rev. D **78**, 034036 (2008) doi:10.1103/PhysRevD.78.034036 [arXiv:0805.3714 [hep-lat]].

[11] D. Vercauteren and H. Verschelde, Phys. Rev. D **82**, 085026 (2010) doi:10.1103/PhysRevD.82.085026 [arXiv:1007.2789 [hep-th]].